Received: 21 July 2021 | Revised: 26 October 2021 | Accepted: 5 November 2021

DOI: 10.1096/fba.2021-00090

FASEB BioAdvances WILEY

RESEARCH ARTICLE

Role of alternatively spliced, pro-survival Protein Kinase C delta VIII (PKCδVIII) in ovarian cancer

Rekha S. Patel[1] | **Rea Rupani**[2] | **Sabrina Impreso**[1] | **Ashley Lui**[2] | **Niketa A. Patel**[1,2]

[1]James A. Haley Veterans Hospital, Tampa, Florida, USA

[2]Department of Molecular Medicine, University of South Florida, Tampa, Florida, USA

Correspondence
Niketa A. Patel, James A. Haley Veterans Hospital, Research Service, 13000 Bruce B. Downs Blvd., Tampa, FL 33612, USA.
Emails: Niketa.Patel@va.gov; Niketa@usf.edu

Abstract

Ovarian cancer is the deadliest malignant disease in women. Protein Kinase C delta (PRKCD; PKCδ) is serine/threonine kinase extensively linked to various cancers. In humans, PKCδ is alternatively spliced to PKCδI and PKCδVIII. However, the specific function of PKCδ splice variants in ovarian cancer has not been elucidated yet. Hence, we evaluated their expression in human ovarian cancer cell lines (OCC): SKOV3 and TOV112D, along with the normal T80 ovarian cells. Our results demonstrate a marked increase in PKCδVIII in OCC compared to normal ovarian cells. Therefore, we elucidated the role of PKCδVIII and the underlying mechanism of its expression in OCC. Using overexpression and knockdown studies, we demonstrate that PKCδVIII increases cellular survival and migration in OCC. Further, overexpression of PKCδVIII in T80 cells resulted in increased expression of Bcl2 and knockdown of PKCδVIII in OCC decreased Bcl2 expression. Using co-immunoprecipitations and immunocytochemistry, we demonstrate nuclear localization of PKCδVIII in OCC and further show increased association of PKCδVIII with Bcl2 and Bcl-xL in OCC. Using PKCδ splicing minigene, mutagenesis, siRNA and antisense oligonucleotides, we demonstrate that increased levels of alternatively spliced PKCδVIII in OCC is regulated by splice factor SRSF2. Finally, we verified that PKCδVIII levels are elevated in samples of human ovarian cancer tissue. The data presented here demonstrate that the alternatively spliced, signaling kinase PKCδVIII is a viable target to develop therapeutics to combat progression of ovarian cancer.

KEYWORDS

alternative splicing, apoptosis, ovarian cancer, PKCδ, SRSF2

Abbreviations: Bad, Bcl2 associated agonist of cell death; Bcl2, B-cell lymphoma 2; Bcl2L1, Bcl2 like 1 (also known as Bcl-x); BH, Bcl2 homology; OCC, Ovarian cancer cell line; PKCδ, Protein Kinase C delta; PKCδI, Protein Kinase C delta I; PKCδVIII, Protein Kinase C delta VIII; SRSF2, Serine-Arginine splice factor 2 (also known as SC35).

1 | INTRODUCTION

Ovarian cancer remains the predominant cause of death from gynecologic malignancy in the United States.[1] This poor outcome is likely related to the fact that most patients are detected with advanced stage disease and widespread peritoneal metastasis. Dysregulation in signaling and metabolic pathways is seen with ovarian cancer where several genes are involved in cross talk resulting in a complex phenomenon. Often, these signaling pathways determine the response to drugs such as paclitaxel and platinum that are administered to treat the ovarian cancer.

The serine/threonine kinase family of Protein Kinase C (PKC) isoforms regulate several signal transduction cascades and are shown to be extensively linked to various cancers. Alterations in expression levels of PKC isoforms are proposed as biomarkers in certain cancers.[2,3] Protein kinase C delta (PKCδ; PRKCD), a member of novel PKC subfamily, plays a central role in cell survival with dual effects: as a mediator of apoptosis and as a promoter of cell survival. The dual functions reported by studies are explained by PKCδ splice variants. Alternative splicing, wherein alternate patterns of exon inclusion/exclusion or choice of 3′ or 5′ splice sites during pre-mRNA splicing, generates more than one protein from the same gene. We demonstrated a novel splice variant in humans and showed that PKCδ alternative splicing produces PKCδI and PKCδVIII, which are switches that determine cell survival and fate. The characterization and function of PKCδVIII was published by our laboratory.[4] PKCδII is the mouse homolog of human PKCδVIII; both are generated by alternative 5′ splice site usage, and their transcripts share >94% sequence homology. We have shown that PKCδII and PKCδVIII function as pro-survival proteins in neurons and adipocytes.[4,5] PKCδ is shown to be involved in tumorigenesis and metastasis in several cancers such as breast, lung, and prostate cancer[6–10]; however, specific function of PKCδ splice variants in any cancer and particularly in ovarian cancer has not been elucidated yet. Since PKCδ regulates apoptosis and survival, we evaluated the expression of PKCδ human splice variants PKCδI and PKCδVIII in human ovarian cancer cells (OCC) SKOV3 and TOV112D along with the normal T80 ovarian cells. Our results demonstrated a marked increase in PKCδVIII in OCC compared to normal ovarian cells which was not recognized thus far.

Cellular pathways mediated by B-cell lymphoma 2 (BCL2) family of proteins determine the balance of apoptosis and survival in cancer. The BCL2 family has BCL2 homology (BH) domains that mediate their pro-survival or pro-apoptotic functions. The antiapoptotic proteins Bcl2 and Bcl-x have the BH4 domain. Bcl-x (also called BCL2-like 1: BCL2L1) is alternatively spliced to generate two variants: Bcl-xL which is antiapoptotic and Bcl-xS which is pro-apoptotic. Bcl2 associated agonist of cell death (BAD), which is pro-apoptotic, contains the BH3 domain. The BCL2 family proteins associate in response to cellular cues and the association of specific partners promote either cellular survival or apoptosis. Bcl2 is held tightly by Bad in a complex. Pro-survival signals promote phosphorylation of Bad resulting in dissociation of this complex. Bcl2 can then associate with Bcl-xL to promote survival and inhibit cytochrome C-mediated apoptosis. Several studies[11–13] have shown that Bcl2 promotes increased survival in ovarian cancer cells. Resistance to drugs in cancer is sometimes conferred by an increase in the pro-survival Bcl2. The link between PKCδVIII and Bcl2 family of proteins is not yet elucidated.

Since elevated expression of PKCδVIII, a pro-survival signaling kinase, may be a significant determinant of life quality and expectancy, we sought to understand the effects of PKCδVIII on cellular and metabolic functions in ovarian cancer and further elucidate the molecular mechanisms that promote its increased expression in ovarian cancer. Understanding the role of alternatively spliced genes contributing to increased survival and proliferation in ovarian cancer cells will lead to development of novel therapeutic approaches.

2 | MATERIALS AND METHODS

2.1 | Cell culture

T80 immortalized normal ovarian epithelial cells were maintained in Roswell Park Memorial Institute (RPMI) 1640 (ThermoFisher Scientific) with 10% Fetal Bovine Serum (FBS) (Atlas Biological), and 1x Penicillin/Streptomycin (Sigma-Aldrich). TOV112D grade 3 endometrioid adenocarcinoma cells were maintained in MCDB105 with 10% FBS, and 1x Pen/Strep. SKOV3 hypodiploid human ovarian adenocarcinoma from grade 1/2 ascites cells were maintained in McCoy's 5A (ThermoFisher) modified medium with L-glutamine, 10% FBS, and 1x Pen/Strep. All human ovarian cancer cells were purchased from ATCC® and T80 normal ovarian cells were a kind gift from Dr. Mildred Acevedo-Duncan (University of South Florida). Cells were grown at 37°C and 5% CO_2.

2.2 | Polymerase chain reaction and SYBR green real-time qPCR

Total RNA was isolated from cells using Trizol™ (ThermoFisher Scientific) as per the manufacturer's

instructions. One microgram of RNA (260/230 > 1.8 and 260/280 >1.8) was used to synthesize cDNA using iScript (1708891, Biorad). One microliter of cDNA was amplified using JumpStart RED Taq Reaction Mix (Sigma, P0982). Primers used in PCR included: PKCδI sense 5′-ACATCCTAGGTACAACAACGGGAC-3′; PKCδI antisense 5′-ACCACGTCCTTCTTCAGACAC-3′; PKCδVIII sense 5′-GCCAACCTCTGCGGCATCA-3′; PKCδVIII antisense 5′-CGTAGGTCCCACTGTTGTCC-3′; Bclx sense 5′-CATGGCAGCAGTAAAGCAAG-3′; Bclx antisense 5′-GCATTGTTCCCATAGAGTTCC-3′; Bcl2 sense 5′-GATGTGATGCCTCTGCGAAG-3′; Bcl2 antisense 5′-CATGCTGATGTCTCTGGAATCT-3′; SRSF2 sense 5′-CCTCGCCCGACACGCTGA-3′; SRSF2 antisense 5′-CCTGGACCGCGAACGAGATCT-3′; GAPDH sense 5′-GATCATCAGCAATGCCTCCT-3′; GAPDH antisense 5′-TGTGGTCATGAGTCCTTCCA-3′. PCR products were run on a 1% agarose gel and imaged in ProteinSimple FluorChemM™. Densitometric analysis was performed using AlphaView Software.

Separately, 1 μl of cDNA was amplified by real-time quantitative PCR using Maxima SYBR Green/Rox qPCR master mix (Thermo Scientific) in an ABI ViiA7 sequence detection system (PE Applied Biosystems) to quantify the relative levels of the transcripts in the samples. Real-time PCR was then performed in triplicate on samples and standards. The plate setup included a standard series, no template control, no RNA control, no reverse transcriptase control, and no amplification control. After primer concentrations were optimized to give the desired standard curve and a single melt curve, relative quotient (RQ) was determined using the $\Delta\Delta C_T$ method with β-actin as the endogenous control and control samples as the calibrator sample.

For absolute quantification (AQ), a standard curve was generated for PKCδVIII. To do so, PKCδVIII-pTracer plasmid was used to obtain a standard curve correlating the amounts (ng) with the threshold cycle number (C_t values). A linear relationship ($r^2 > 0.96$) was obtained for PKCδVIII. Real-time qPCR was then performed on samples and standards in triplicates. Samples were normalized to β-actin for absolute quantification of PKCδVIII expression levels.

2.3 | Western blot analysis

Cell lysates (50 μg) were harvested using lysis buffer (Cell Signaling 9803S) containing 10% protease/phosphatase inhibitor (Pierce A32957, A32953) then sonicated briefly. Samples were separated on a 10% SDS-PAGE gel. Proteins were electrophoretically transferred to nitrocellulose membranes and blocked with 5% nonfat dried milk in Tris-Buffered Saline with 0.05% Tween 20 (TBST). Membranes were probed with antibodies against PKCδI (Santacruz, sc213 or Cell signaling), PKCδVIII (specific antibody developed by our lab and verified in a previous publication[4]), pBad (Cell Signaling 9295S), Bad (Cell Signaling 9292S), Bcl-xL (Cell Signaling, 2764), Bcl2 (Cell Signaling 15071S), p-β-catenin (Cell Signaling, 9561), β-catenin (R&D, mab1329), β-Actin (Sigma, A3884), GAPDH (Santacruz, sc25778). Secondary HRP antibodies were purchased from Bio-Rad for rabbit (5196-2504) and mouse (0300-0108P). Incubation with chemiluminescence (Pierce 32109) was used for detection and images were digitally captured using in ProteinSimple FluorChem M™. Densitometric analysis was performed using AlphaView Software.

2.4 | Transfection of PKCδVIII plasmid and antisense oligonucleotides

The pTracer-PKCδVIII plasmid was cloned and verified by sequencing as described in our previous publications.[4,14] The 20-mer antisense oligonucleotide masking the SRSF2 binding site on PKCδ mRNA (ASO) is 2′-methoxyethyl- modified, RNase-H resistant and was synthesized by Ionis Pharmaceuticals, CA along with the scrambled control. Cells were transfected with 2 μg of pTracer-PKCδVIII plasmid or the ASO for 48 h using Lipofectamine 3000 reagent (ThermoFisher) per manufacturer's instructions. Control cells were transfected using Lipofectamine 3000 alone or control ASO as per experimental setup. Total RNA was harvested and PCR was performed as described above.

2.5 | Knockdown of PKCδVIII or SRSF2

PKCδVIII siRNA was custom designed (validated as described in Ref. [14]) to target PKCδVIII pre-mRNA, and purchased from ThermoFisher Scientific: PKCδVIII siRNA (ID: 10620110). SRSF2 siRNA (ThermoFisher ID:4392420, previously validated for specificity using three siRNAs and elimination of off-target effects[14]) was purchased from ThermoFisher Scientific along with nonspecific siRNA used in experiments as control. Cells were transfected with 25 nM PKCδVIII siRNA or 50 nM SRSF2 siRNA along with control siRNA for 48 h using RNAiMax reagent (ThermoFisher) per manufacturer's instructions. Total RNA was harvested and PCR was performed as described above or whole cell lysates were analyzed using Western blot as described above to confirm the depletion.

2.6 | AOPI cellular survival assay

Cells were grown in a 12-well plate and PKCδVIII was overexpressed as described above. Cells were treated with 25 μg/ml etoposide for 18 h. Cells were then trypsinized and washed once with PBS. The cell pellet (containing one million cells) was resuspended in 500 μl PBS and fixed by slow, drop-wise addition of 4.5mL ice-cold 70% ethanol while gently vortexing. Samples were incubated overnight at 4°C to complete fixation and then stored at −20°C until stained. A fresh solution of Propidium Iodide (1 mg/ml, ViaStain™ CS1-0109) and RNase A (2mg/ml, ThermoFisher EN0531) diluted in water. Fixed cells were centrifuged at 1000 rpm for 5 min. Cell pellet was washed twice with PBS and pellet was resuspended in 50 μl PI/RNase A solution and incubated at room temperature for 5 min. One milliliter PBS was added and samples were divided to create unstained negative control for analysis. Acridine Orange (ViaStain™ CS2-0106) was added (1:1) to samples for staining and incubated at 37°C for 30 min then analyzed on the Nexcelom K2 cellometer.

2.7 | Cell migration by scratch assay

Cells were grown to confluency in 35-mm dishes with μ-Dish inserts (Ibidi solutions™, 81176) to make consistent and reproducible 500μm gaps. PKCδVIII was overexpressed in T80 cells or expression was knocked down in OCC for 48 h. The inserts were then removed and imaged on the Keyence BZx-810 microscope at 4x magnification. Images were taken at the same location saved into the Keyence BZx-810 microscope with images taken at 0, 24, and 48 h. Analysis of done measuring empty area between cells in μm^2 using the FastTrack A1 software (Ibidi solutions™).

2.8 | Cell migration assay

Transwell cell migration assays were performed using BD Falcon Cell Culture Inserts in a 24-well plate. Ovarian cancer cells were plated in the upper insert in their respective serum-free medium and the outer, bottom chamber was filled with 300 μl of respective medium containing 10% FBS. The ovarian cancer cells with and without the PKCδVIII siRNA were allowed to migrate for 18 h. After 18 h, the cells that migrated to the bottom well were fixed and stained using crystal violet and imaged on Keyence BZx-810 microscope. The number of cells were counted using the automated Keyence software analysis module.

2.9 | Co-immunoprecipitation assay

Cells were harvested and 200 μg of lysate was used for co-immunoprecipitation assay. Lysates were rocked with Protein A/G Agarose (Santa Cruzsc2003) for 30 min at 4°C to clear nonspecific binding and centrifuged at 2000 rpm for 1 min. The supernatant was rocked with 2 μg Bcl2-agarose antibody (Santa Cruz sc7382AC), Bcl-xL-agarose antibody (Santa Cruz sc8392AC) or Bad-agarose antibody (Santa Cruz, sc8044AC) overnight at 4°C and pellet was washed and resuspended in Laemmli buffer followed by Western blot analysis as described above.

2.10 | Immunocytochemistry

Ovarian cells were plated into a 12-well plate as described above. Cells were fixed with 4% paraformaldehyde for 30 min at room temperature and blocked with 1% bovine serum albumin in PBS for 1 h. Cells were incubated in primary antibodies against Bcl2 (1:100), Bad (1:100), Bcl-xL (1:100), and PKCδVIII (1:50). Cells were rocked overnight at 4°C. Cells were then washed with PBS and rocked in the dark for 1 hour in Alexafluor 488 and Alexafluor 577 secondary antibodies (1:1000, Invitrogen). Cells were briefly rinsed with PBS and stained with DAPI mounting media. Images were captured using Keyence BZx-810 microscope and analyzed using Keyence Analyzer software.

2.11 | WST cell viability assay

Cells were grown to in 35-mm dishes and PKCδVIII siRNA was transfected as described above. WST-1 (Roche Molecular Biochemicals, IN) was diluted to a final concentration of 10% (v/v) in serum-free cell media. Cells were incubated for 2 h at 37°C. The formazon dye produced by viable cells was quantified using a spectrophotometer set at a wavelength of 440 nm, and absorbance was recorded for each well using reference wavelength of 690 nm.

2.12 | BrdU proliferation assay

BrdU (Millipore, 2750) was diluted to 100 μM stock concentration in PBS, then diluted 1:10 in culture media. Cells were washed with PBS before incubated in BrdU media for 2 h. Cells were then fixed in 4% paraformaldehyde for 20 min at room temperature then blocked for 30 min at room temperature. One milliliter of antibody staining buffer with anti-BrdU primary antibody was added and incubated overnight at room temperature. Peroxidase- secondary antibody was added for 1 h at room temperature

then Peroxidase substrate was added for 30 min at room temperature. Positive wells were visibly blue and intensities were measured by spectrophotometer readings at 450/540 nm.

2.13 | Construction of pSPL3_PKCδ and pSPL3_PKCδ**SRSF2 Minigenes

The pSPL3_PKCδ splicing minigene was constructed as described in our previous publication.[14] Briefly, PKCδ exon 10 and its flanking 3′ intronic sequence (containing the branch point and 3′ splice site) and 5′ intronic sequences (containing flanking 5′ intronic sequence that includes 5′ splice site I and splice site II) were cloned into the multiple cloning site of the pSPL3 splicing vector between the splice donor (SD) exon and splice acceptor (SA) exon. The resulting splicing minigene was verified by restriction digestion and sequencing. To generate the pSPL3_PKCδ**SRSF2 minigene, the SRSF2 cis-element (sequence: ggccaaag) identified near 5′ splice site II of exon 10 of PKCδ pre-mRNA, was mutated in the pSPL3_PKCδ minigene to "tagcccata" using QuikChange site-directed mutagenesis kit (Stratagene), which allows for blue/white screening per the manufacturer's instructions. The mutated minigene, pSPL3_PKCδ**SRSF2, was verified by sequencing (published in Ref. [14]). Two micrograms of pSPL3_PKCδ or pSPL3_PKCδ**SRSF2 minigene was transfected into cells, total RNA was isolated and PCR was performed to visualize splicing of the minigene using primers SD 5'-TCTGAGTCACCTGGACAACC-3' and SA 5'-CACCTGAGGAGTGAATTGGTC-3'.

2.14 | Statistical analysis

All experiments were repeated 3–5 times as biological replicates and experimental samples run in triplicate to ensure reproducibility of results. Analyses were performed using PRISM^{TM} software and analyzed using two-tailed Student's *t*-test, one-way or two-way ANOVA as indicated in figure legends. $*p < 0.05$, $**p < 0.01$, and $***p < 0.001$ were used as significant measures.

3 | RESULTS

3.1 | PKCδVIII levels are increased in ovarian cancer cells

In humans, PRKCD gene (i.e., PKCδ) is alternatively spliced to PKCδI and PKCδVIII mRNA[4] via utilization of alternate 5′ splice sites on exon 10 as shown in schematic of Figure 1A. We evaluated the expression of PKCδ splice variants PKCδI and PKCδVIII in normal immortalized human ovarian epithelial T80 cells and human ovarian cancer cells (OCC) SKOV3 and TOV112D. Total RNA was isolated for real-time SYBR Green quantitative PCR using primers specific for PKCδI and PKCδVIII. Simultaneously, whole cell lysates were analyzed by Western blot using antibody against PKCδI (Cell Signaling) and PKCδVIII-specific antibody (raised by Patel lab as published in Ref. [4]). The levels of PKCδI were not significantly different between OCC and normal T80 cells. Results (Figure 1B,C) demonstrate a 7-fold increased expression of PKCδVIII in SKOV3 compared to T80 while TOV112D had 12-fold increased expression of PKCδVIII compared to T80 cells.

3.2 | Increased expression of PKCδVIII in ovarian cells promotes cellular survival

Since our results showed increased expression of PKCδVIII in ovarian cancer cells compared to normal ovarian cells, we sought to evaluate the impact of increased levels of PKCδVIII on cell survival in ovarian cells. Hence, we overexpressed PKCδVIII in T80 cells. Overexpression was confirmed by PCR using primers that detected PKCδI and PKCδVIII simultaneously (Figure 2A). We evaluated cell survival in response to etoposide, an inducer of apoptosis that is also used in cancer treatment regimens, using Acridine Orange/Propidium Iodide (AOPI) staining. After 48 h of PKCδVIII overexpression, medium was changed and 25μg/ml etoposide was added for 18 h. The live and dead cells were measured on a Cellometer (Nexcelom). Briefly, PI stains cells with compromised membranes and hence fluorescence by AO is reduced in dead cells. Results (Figure 2B) demonstrate that overexpression of PKCδVIII protects cells against etoposide-induced apoptosis.

3.3 | PKCδVIII increases expression of pro-survival proteins Bcl2 and Bcl-xL

Prior research has demonstrated that B-cell leukemia-2 gene product (Bcl2) family of survival proteins: Bcl2 and Bcl-xL promote survival in cancer cells.[15] Hence, we evaluated their levels in T80, SKOV3 and TOV112D cells. Total RNA was isolated and used in SYBR Green real-time qPCR analysis. Results (Figure 3A) indicate significantly higher expression of Bcl2 and Bcl-xL in SKOV3 and TOV112D concurrent with PKCδVIII expression compared to T80 cells. Since increased survival mediated by Bcl2 and Bcl-xL is implicated in cancer cells, we evaluated the levels of Bcl2 and Bcl-xL in PKCδVIII overexpressing T80 cells. Results (Figure 3B,C) show that overexpression of PKCδVIII

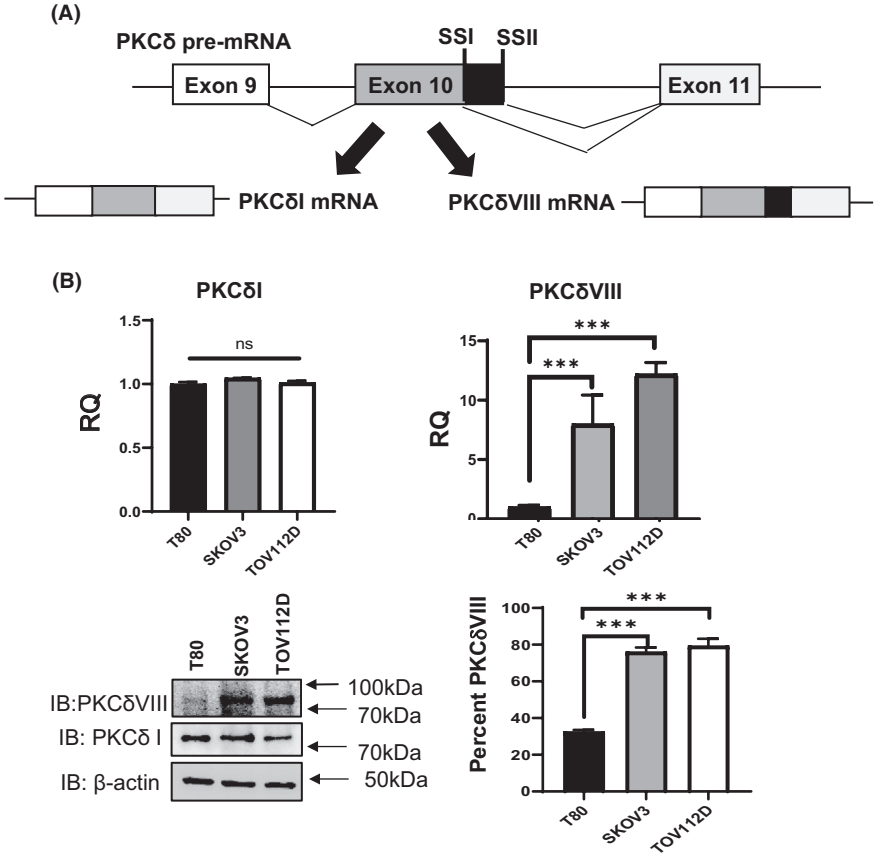

FIGURE 1 PKCδVIII is increased in ovarian cancer cells. (A) Schematic depicts PKCδ pre-mRNA alternative splicing which produces PKCδI mRNA (via utilization of 5′ splice site I (SSI) of exon 10) and PKCδVIII mRNA (via utilization of 5′ splice site II (SSII) of exon 10). (B) Total RNA was isolated from T80, SKOV3, and TOV112D ovarian cells followed by real-time SYBR Green qPCR analysis using primers specific to PKCδVIII, PKCδI, and β-actin (internal control). Graph shows relative quantification (RQ) for PKCδI and PKCδVIII with T80 set as reference. The experiments were independently repeated five times with similar results. Statistical analysis was performed using one-way ANOVA; *** $p < 0.001$. (C) Western blot analysis was performed on whole cell lysates and probed using antibodies against PKCδVIII, PKCδI, and β-actin as indicated in the figure. Densitometric analysis of individual bands for each protein were normalized to β-actin and percent PKCδVIII (PKCδVIII expression in total PKCδ) was calculated using the following equation: percent PKCδVIII = [PKCδVIII / (PKCδVIII + PKCδI)] × 100. Statistical analysis was performed using one-way ANOVA; ***$p < 0.001$

increased Bcl2 levels. Interestingly, we observe increased expression of Bcl-xL, with no significant change in Bcl-xS levels, in PKCδVIII overexpressing T80 cells. These results demonstrate that increased expression of PKCδVIII promotes genes in survival pathways in ovarian cells.

3.4 | Ovarian cells overexpressing PKCδVIII have increased cellular migration

Next, we determined the migration of T80 cells overexpressing PKCδVIII compared to control T80 cells. Scratch assay is an established method to measure cell migration *in vitro*.[16] Ibidi culture inserts were used to create cell-free gaps which are reproducible. T80 cells were plated in 35-mm dishes with inserts and transfected with 2 μg of pTracer-PKCδVIII as described above. After 24 h insert is removed and images were taken at 24 h using Keyence BZx810. Quantification of migration is achieved by FastTrack A1 Image analysis software (Ibidi solutions™). Our results (Figure 4A,B) demonstrate that PKCδVIII overexpression accelerated rate of migration in T80 cells.

3.5 | PKCδVIII associates with Bcl2 in ovarian cells

Since PKCδVIII is a pro-survival kinase and our results above showed that its expression is increased in ovarian cancer cells, we sought to elucidate the survival pathway through which PKCδVIII mediated survival in ovarian cancer cells. We performed a co-immunoprecipitation in T80 cells along with T80 cells overexpressing PKCδVIII. Whole cell lysates were harvested, and the PKCδVIII-specific antibody was used to immunoprecipitate the

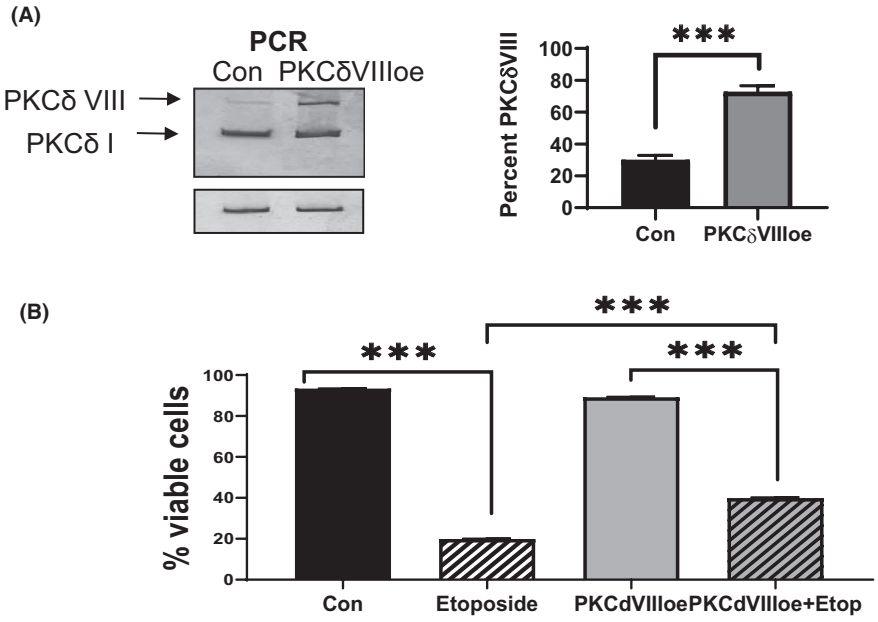

FIGURE 2 Overexpression of PKCδVIII in T80 cells promotes cellular survival. (A) 2μg of pTracer-PKCδVIII was transfected in T80 cells for 48 h. (A) RNA was isolated and PCR was performed using primers that simultaneously detect both PKCδ variants. Five percent of the products were separated by PAGE and silver stained for visualization. The experiments were independently repeated five times with similar results. Graph shows percent PKCδVIII (PKCδVIII expression in total PKCδ) that was calculated using the following equation: percent PKCδVIII = [PKCδVIII / (PKCδVIII + PKCδI)] × 100. Statistical analysis was performed using *t*-test; ***$p < 0.001$. (B) 48 h after pTracer-PKCδVIII transfection, T80 cells were treated with 25 μg/ml etoposide for 18 hours. Cells were fixed and stained with acridine orange (AO) and propidium iodide (PI) and viability of cells was analyzed using a cellometer. The experiments were independently repeated four times with similar results. Statistical analysis was performed using one-way ANOVA; ***$p < 0.001$

associated proteins. Western blot was then performed for proteins associated with survival in ovarian cancer. Our results (Figure 5A,B) showed high levels of association of PKCδVIII with Bcl2, Bcl-xL, and Bad. Bax, Bak, Caspase-3, Caspase-9, PARP, and XIAP were not detected in the co-immunoprecipitation indicating that these proteins of the apoptosis pathway did not associate with PKCδVIII.

Based on these results, we sought to validate that PKCδVIII was associated with the Bcl2, Bcl-xL, Bad protein complexes. Cell survival is mediated by Bcl2 and Bcl-xL which inhibit the activity of Bax-Bak as well as through inhibition of the cytochrome C-mediated caspase cascade. Bcl2 is sequestered by hypo-phosphorylated Bad which decreases the ability of Bcl2 to associate with Bclx-L to promote survival. Hence, whole cell lysates were harvested from T80 and T80 overexpressing PKCδVIII followed by immunoprecipitation using antibodies against Bcl2, Bcl-xL or Bad. Western blot was then performed to evaluate the associated proteins. Figure 5A shows the Western blot with the input lysate. Results from Bcl2 immunoprecipitation (Figure 5C) showed PKCδVIII and Bcl-xL associated with Bcl2 in T80 cells. In PKCδVIII-overexpressing T80 cells, the association between Bcl2 and PKCδVIII as well as Bcl2 and Bcl-xL is dramatically increased. A similar association was seen in Bcl-xL immunoprecipitated T80 cells (Figure 5D) and increased levels of Bcl2 and PKCδVIII associated with Bcl-xL in PKCδVIII-overexpressing T80 cells. Interestingly in PKCδVIII-overexpressing T80 cells, results from Bad immunoprecipitation (Figure 5E) showed a significant decrease in association of Bcl2 and Bcl-xL with Bad while PKCδVIII association with Bad did not change significantly. As seen in the Western blots of the lysates (panels in Figure 5A) the phosphorylation of Bad (S112) was significantly increased in PKCδVIII-overexpressing T80 cells. PKCδVIII did not associate with Bax or Bak (not shown). These results demonstrate that increased expression of PKCδVIII in ovarian cells promotes the association of survival complex Bcl2-Bcl-xL with simultaneous dissociation of Bcl2 and Bad complex that is concurrent with increased survival and migration.

3.6 | PKCδVIII colocalizes with Bcl2 and Bcl-xL

To visualize the association and localization in situ, we performed immunocytochemistry in T80, SKOV3 and TOV112D cells. Using an antibody specific for PKCδVIII, results (Figure 5E) demonstrate that PKCδVIII is expressed both in the cytoplasm and nucleus with higher levels of expression observed in SKOV3 and TOV112D cells compared

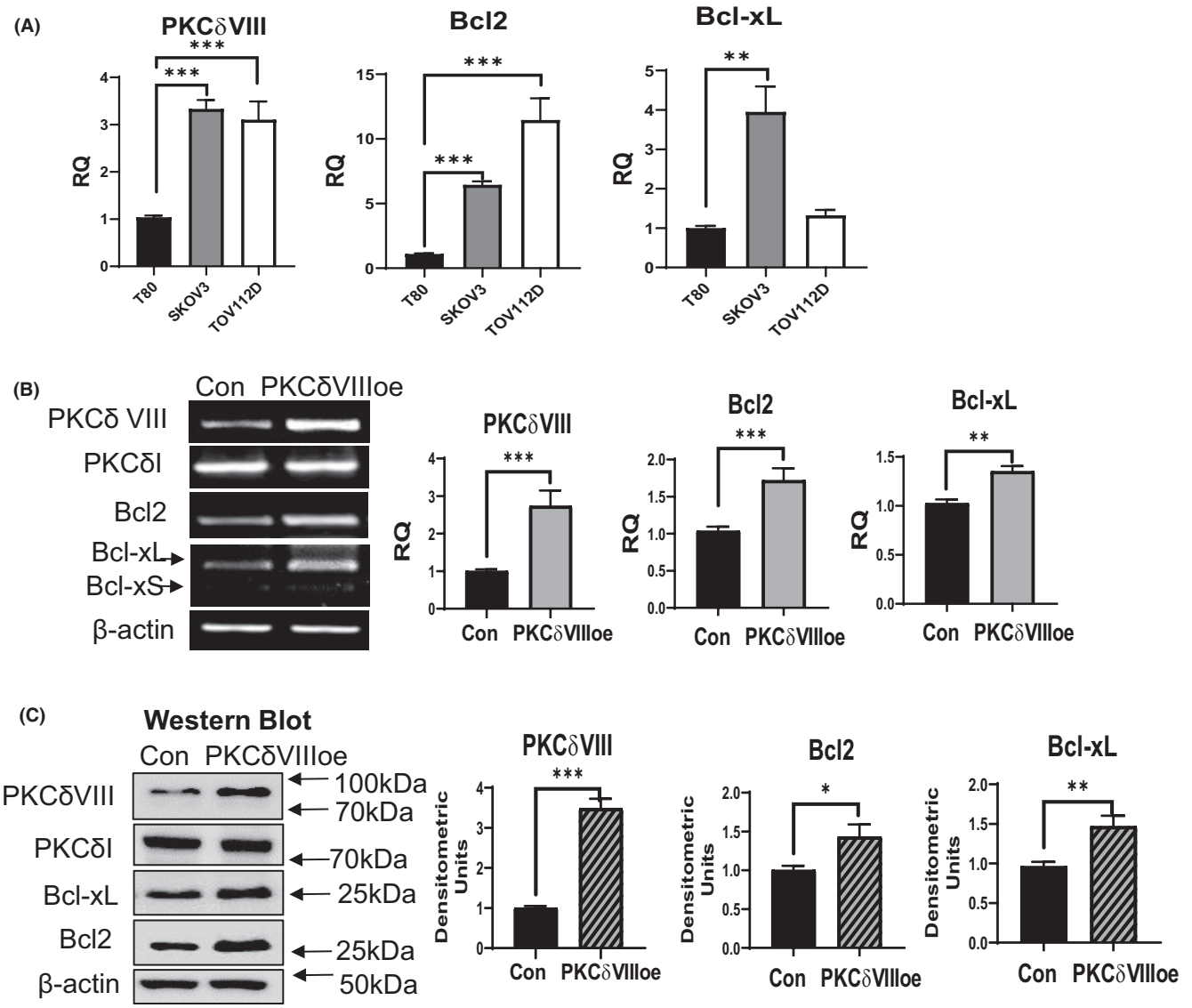

FIGURE 3 Overexpression of PKCδVIII in T80 cells increases Bcl2 and Bcl-xL. (A) RNA was isolated and endogenous levels of PKCδVIII, Bcl2, and Bcl-xL in T80, SKOV3, and TOV112D cells were determined by real-time SYBR Green qPCR. Graph shows relative quantification (RQ) for Bcl2, Bcl-xL, and PKCδVIII with T80 set as reference. The experiments were independently repeated five times with similar results. Statistical analysis was performed using one-way ANOVA; $*p < 0.05$, $**p < 0.01$. (B) 2 μg of pTracer-PKCδVIII was transfected in T80 cells for 48 h. RNA was isolated and PCR was performed using primers for PKCδI, PKCδVIII, Bcl2, Bcl-x (primer pair simultaneously detects Bcl-xL and Bcl-xS) and β-actin. PCR products were run on a 1% agarose gel and stained using ethidium bromide. Graphs show relative quantification of PKCδVIII, Bcl2, and Bcl-xL normalized to β-actin with control set as reference. The experiments were independently repeated four times with similar results. Statistical analysis was performed using *t*-test; $**p < 0.01$ and $***p < 0.001$. (C) 2 μg of pTracer-PKCδVIII was transfected in T80 cells for 48 h and whole cell lysates were analyzed using Western blot. Membranes were probed using antibodies as indicated in figure. Graphs show densitometric analysis of PKCδVIII, Bcl2 and Bcl-xL normalized to β-actin. The experiments were independently repeated three times with similar results. Statistical analysis was performed using *t*-test; $*p < 0.05$ and $**p < 0.01$

to T80. Interestingly, PKCδVIII expression is higher in nucleus in the cancer cell lines SKOV3 and TOV112D. The results further demonstrate that PKCδVIII is colocalized with Bcl2 and Bcl-xL in nucleus and PKCδVIII colocalizes with Bad in the cytoplasm. Using Pearson's coefficient for analysis, our results demonstrate that the colocalization of PKCδVIII with Bcl2 and Bcl-xL is higher in cancer cells SKOV3 and TOV112D compared to normal T80 cells.

3.7 | Depletion of PKCδVIII decreases Bcl2 in ovarian cancer cells

Since our results above showed that PKCδVIII promoted survival pathways, we evaluated whether depletion of PKCδVIII in ovarian cancer cells affected cellular migration and survival genes. Previously, we validated a PKCδVIII-specific siRNA that depleted the cells of PKCδVIII and did

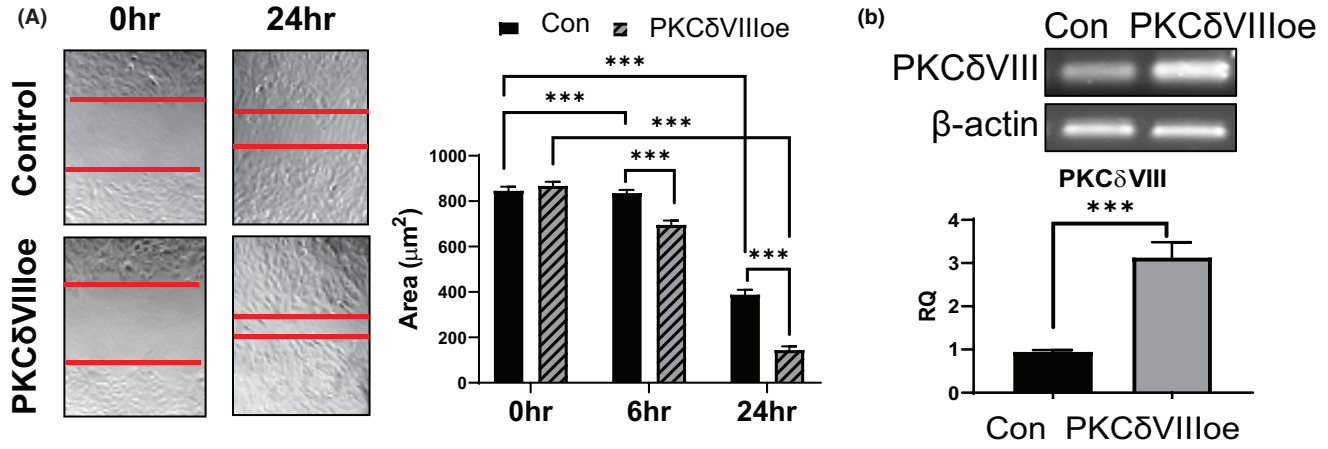

FIGURE 4 Overexpression of PKCδVIII in T80 increases cell migration. (A) T80 cells grown to confluency with μ-Dish inserts (Ibidi solutions, 81176) and were transfected with 2 μg pTracer-PKCδVIII plasmid for 48 h. Inserts were removed to make consistent gaps and cells were imaged at 0, 6, and 24 h. The red lines are drawn on the image to aid in visualization of the edges of the gaps. The cells were imaged using Keyence BZx-810 microscope and analysis of gap area between cells (μm^2) was quantified using FastTrack A1 software (Ibidi solutions™). (B) RNA was then isolated from the cells and PCR performed using PKCδVIII specific primers. The products were separated on a 1% agarose gel and stained using ethidium bromide. Graph shows relative quantification of PKCδVIII normalized to β-actin with control set as reference. The experiments were independently repeated three times with similar results. Statistical analysis was performed using two-way ANOVA; *** $p < 0.001$

not affect PKCδI expression.[14] Hence, we transfected 25nM PKCδVIII siRNA (and a nonspecific siRNA (control) in SKOV3 and TOV112D cells for 48 h. Total RNA was isolated for real-time quantitative SYBR Green PCR using primers specific for PKCδI, PKCδVIII, and Bcl2. Simultaneously, whole cell lysates were harvested for Western blot analysis using antibodies against PKCδI (Cell Signaling), PKCδVIII (specific antibody as published in Ref. [14]) or Bcl2 (Cell Signaling). Results (Figure 6A,B) demonstrate a significant decrease of PKCδVIII levels in PKCδVIII-depleted SKOV3 ($SKOV3_{PKC\delta VIIIsi}$) compared to SKOV3 (control siRNA) as well as in PKCδVIII-depleted TOV112D ($TOV112D_{PKC\delta VIIIsi}$) compared to TOV112D (control siRNA). Further, our results demonstrate a concurrent decrease in Bcl2 expression with depletion of PKCδVIII. The levels of PKCδI remained unchanged with knockdown of PKCδVIII.

3.8 | Depletion of PKCδVIII decreases cellular migration in ovarian cancer cells

Next, we determined cellular migration using the scratch assay (as described above in Figure 2) in SKOV3, $SKOV3_{PKC\delta VIIIsi}$, TOV112D, $TOV112D_{PKC\delta VIIIsi}$. Results (Figure 6C) demonstrate that $SKOV3_{PKC\delta VIIIsi}$ and $TOV112D_{PKC\delta VIIIsi}$ have significantly lower migration rates compared to control SKOV3 and TOV112D, respectively, as determined by slower closure of wound gap. To further validate that PKCδVIII influenced cell migration, we performed the transwell cell migration assay for 18 h in SKOV3, $SKOV3_{PKC\delta VIIIsi}$, TOV112D, $TOV112D_{PKC\delta VIIIsi}$. Results (Figure 6D) demonstrate that $SKOV3_{PKC\delta VIIIsi}$ and $TOV112D_{PKC\delta VIIIsi}$ have significantly lower cell migration rates compared to control SKOV3 and TOV112D, respectively, as determined by the lower number of cells migrating through the physical barrier toward the chemo-attractant (FBS). Results from these assays indicate that PKCδVIII affects the migration of ovarian cancer cells.

3.9 | Depletion of PKCδVIII decreases cell survival in ovarian cancer cells

Separately, WST-1 assay was used to determine cell survival in PKCδVIII depleted SKOV3 and TOV112D cells as described above. After 48 hours of PKCδVIII-siRNA transfection, WST-1 assay was performed. The formazan dye produced by viable cells was quantified according to manufacturer's instructions. Results (Figure 6E) demonstrate a decrease in cell survival in $SKOV3_{PKC\delta VIIIsi}$ and $TOV112D_{PKC\delta VIIIsi}$ compared to SKOV3 and TOV112D, respectively.

3.10 | Depletion of PKCδVIII decreases cell proliferation in ovarian cancer cells

Next, we determined the effect of depleting PKCδVIII on proliferation of ovarian cancer cells. SKOV3 and TOV112D were depleted of PKCδVIII using its specific siRNA as described above in a 48-well plate where each group was performed in triplicate. After 48 h, 100 μl BrdU

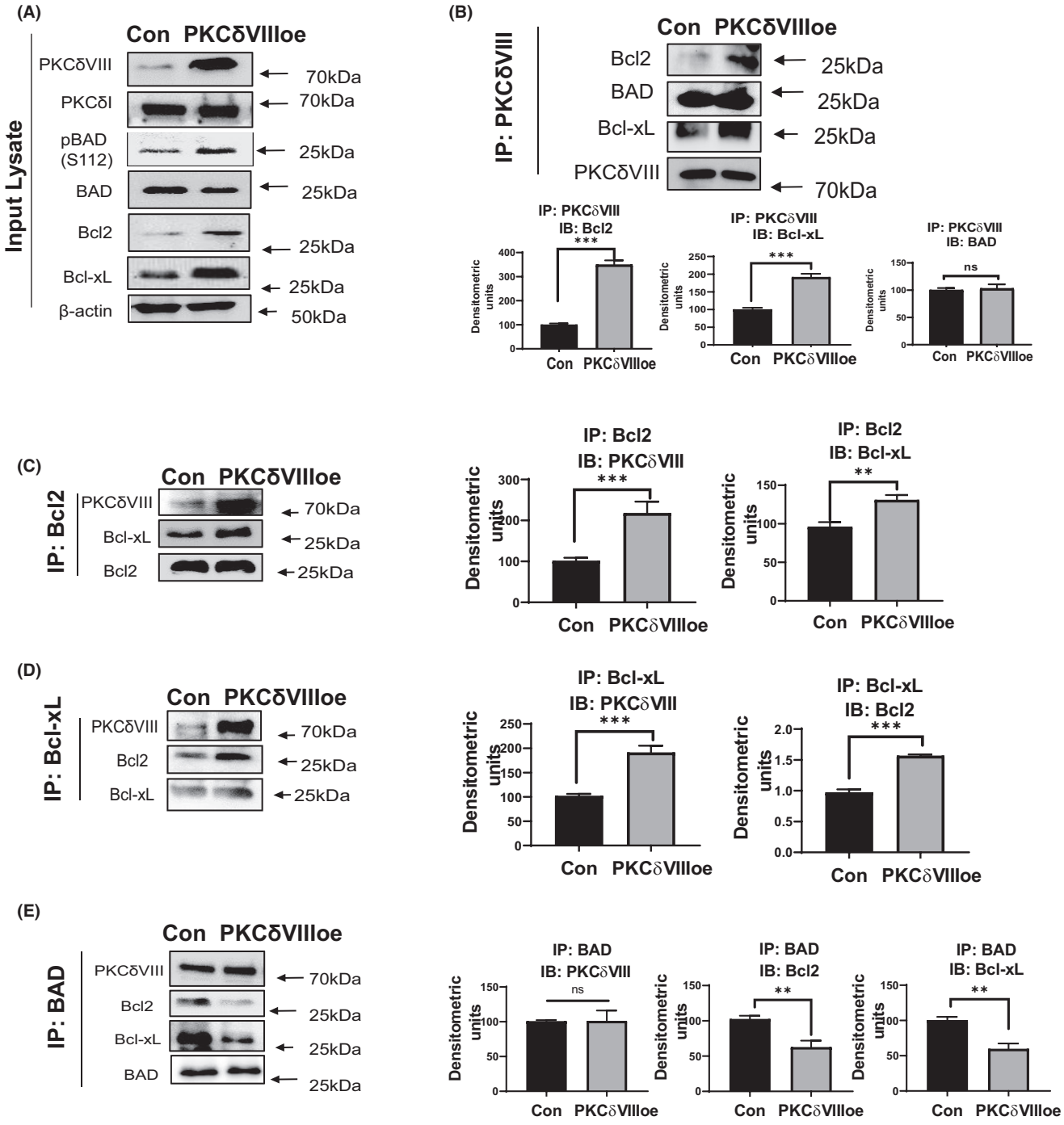

FIGURE 5 PKCδVIII associates with Bcl2 and Bcl-xL in ovarian cells. Two micrograms of pTracer-PKCδVIII was transfected in T80 cells for 48 h. (A) Western blot analysis was performed on input lysates and probed using antibodies as indicated. Coimmunoprecipitation assay was performed on the cell lysates using antibodies against (B) PKCδVIII (IP: PKCδVIII, $n = 4$) (C) Bcl2 (IP: Bcl2, $n = 3$), (D) Bcl-xL (IP: Bcl-xL, $n = 3$), and (e) BAD (IP:BAD, $n = 4$). Western blot analysis was then performed on the immunoprecipitated samples (IP) using antibodies against PKCδVIII, Bcl2, Bcl-xL, and Bad as indicated in the figure. Graphs show densitometric analysis of individual band normalized to immunoprecipitated antibody target. Statistical analysis was performed using *t*-test; $^{**}p < 0.01$, $^{***}p < 0.001$, and ns = not significant. The experiments were independently repeated three times with similar results. (F) Immunocytochemistry was performed on T80, SKOV3, and TOV112D ovarian cells by fixing and staining cells using antibodies against PKCδVIII, Bcl2, Bcl-xL, Bad, and DAPI (for nucleus) and as indicated in the figure. Cells were imaged using a Keyence BZx-810 microscope and Pearson's colocalization was calculated using Keyence Analyzer software. The experiments were independently repeated four times with similar results. Statistical analysis was performed using one-way ANOVA; $^{***}p < 0.001$ and ns = not significant

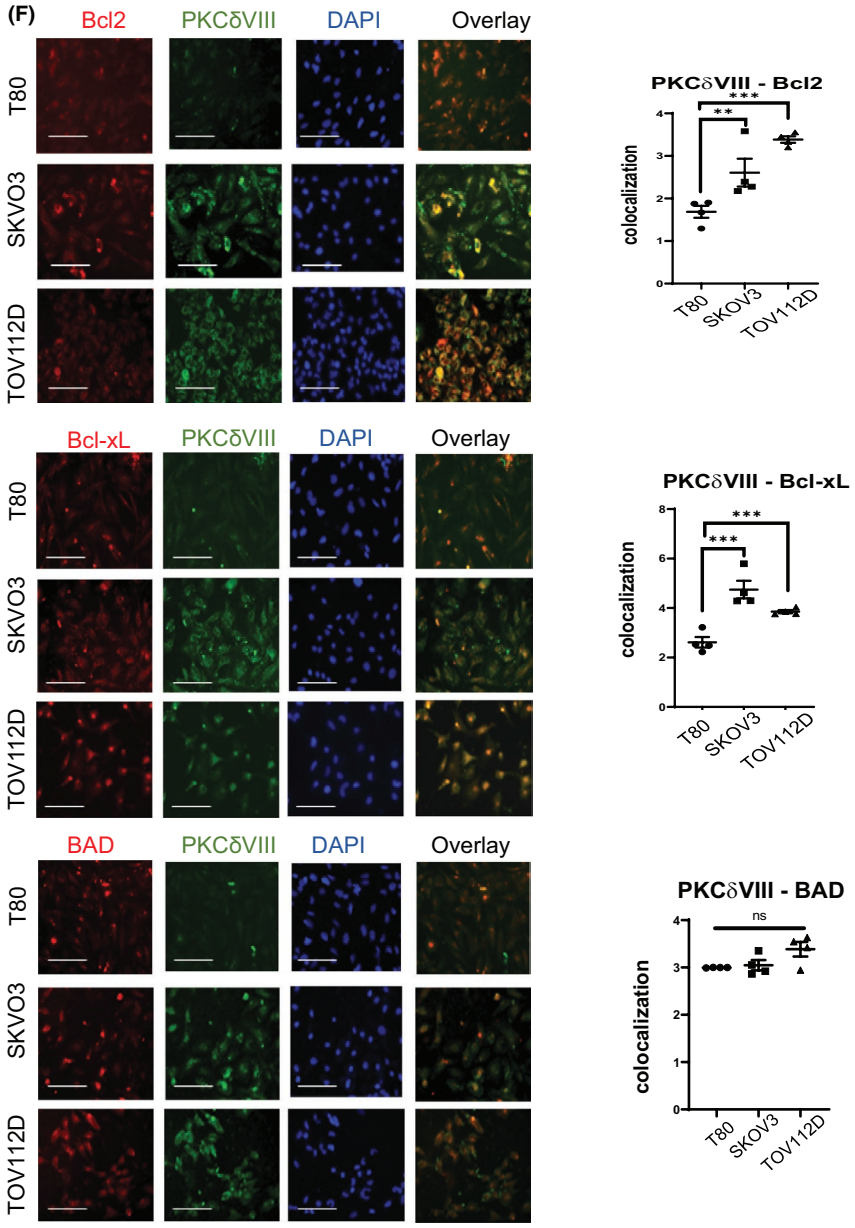

FIGURE 5 (Continued)

was added to determine cellular proliferation. The BrdU incorporated into the cells was measured using peroxidase conjugate and represented the percent of proliferating cells. Results (Figure 6F) demonstrate that depleting PKCδVIII from SKVO3 or TOV112D cells resulted in decreased proliferation compared to their respective controls.

3.11 | Alternative splicing of PRKCD promotes higher expression of PKCδVIII via SRSF2 in ovarian cancer cells

We sought to evaluate the molecular events resulting in increased alternative splicing and expression of PKCδVIII in SKOV3 and TOV112D. Previously,[4] we demonstrated that alternative splicing of the PRKCD gene in humans results in two variants: PKCδI and PKCδVIII as shown in the schematic (Figure 1A above). Using overexpression and knockdown studies, we had previously demonstrated that the splice factor SRSF2 (also known as SC35) regulated the expression of PKCδVIII in neuronal cells.[14] In this study using gel PCR, our results (Figure 7A) demonstrate a marked increase in SRSF2 in SKOV3 and TOV112D cancer cells compared to T80 normal cells which were concurrent with increased expression of PKCδVIII. To evaluate whether increased expression of SRSF2 in the cancer environment resulted in increase in the pro-survival PKCδVIII expression, we performed knockdown studies. SRSF2 was depleted by transfecting SRSF2 siRNA along with its control siRNA into SKOV3 and

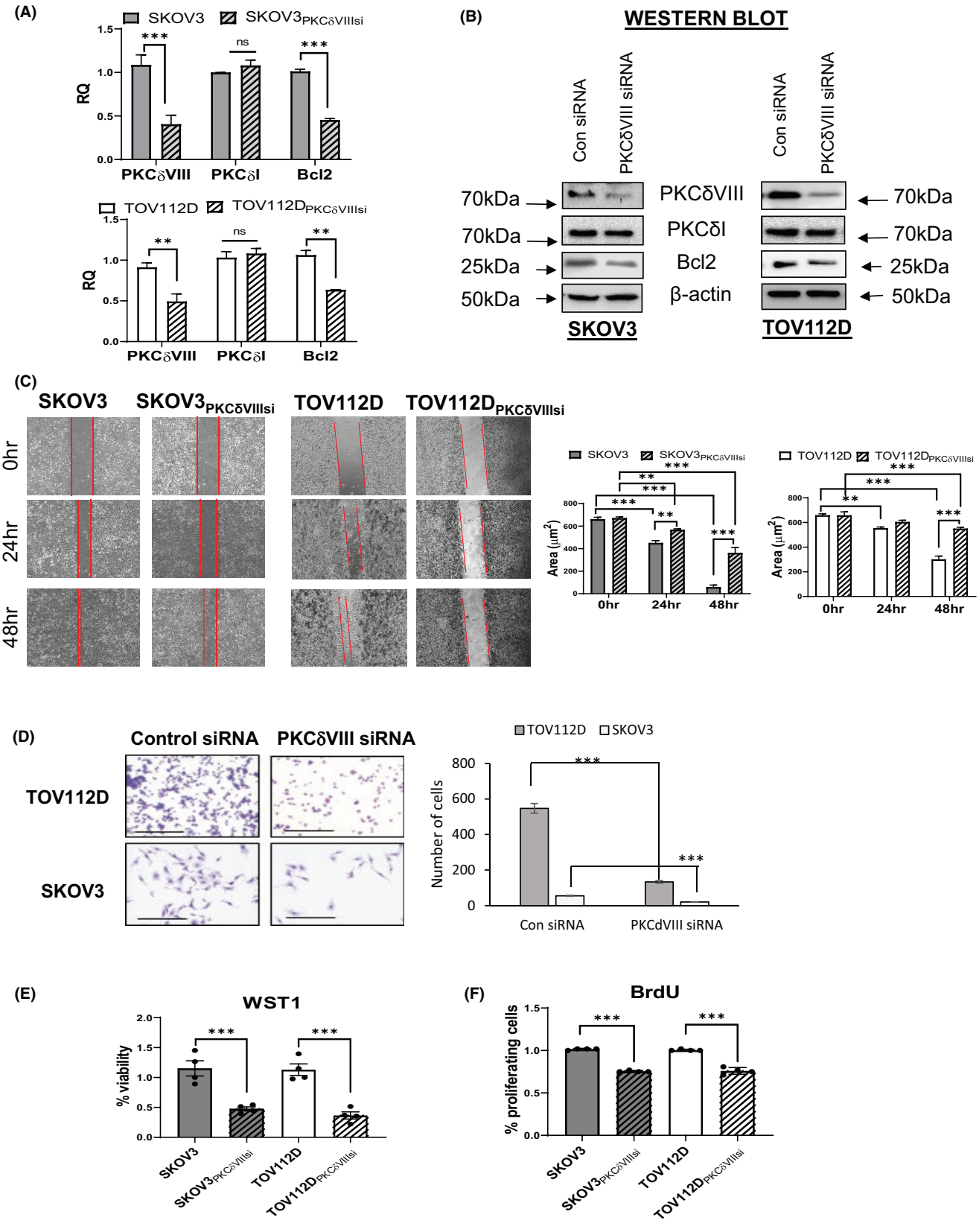

TOV112D for 48 h. Total RNA was harvested and real-time SYBR Green qPCR was performed using primers for SRSF2, PKCδVIII, and PKCδI. Our results (Figure 7B) demonstrate that depletion of SRSF2 in SKOV3 and TOV112D significantly decreased the expression of PKCδVIII; PKCδI levels did not change significantly with depletion of SRSF2.

FIGURE 6 Depletion of PKCδVIII in ovarian cancer cells decreases Bcl2 and cellular migration, viability, and proliferation. 25 nM of PKCδVIII specific siRNA was transfected in SKOV3 ($SKOV3_{PKCδVIIIsi}$) and TOV112D ($TOV112D_{PKCδVIIIsi}$) or 25nM control siRNA (control) was transfected into the cells for 48 h. (A) RNA was isolated and Real-time SYBR Green qPCR was performed for PKCδVIII, PKCδI, Bcl2, and β-actin. Graphs show relative quantification of PKCδVIII, Bcl2, and Bcl-xL normalized to β-actin with control set as reference. The experiments were independently repeated four times with similar results. Statistical analysis was performed using *t*-test; $^{**}p < 0.01$, $^{***}p < 0.001$ and ns = not significant. (B) Whole cell lysates were harvested and Western blot was performed using antibodies as indicated. The experiments were independently repeated four times with similar results. (C) SKOV3 and TOV112D were grown to confluency with μ-Dish inserts (Ibidi solutions, 81176), PKCδVIII was depleted by siRNA transfection for 48 h. Inserts were removed to make consistent gaps and cells were imaged at 0, 24, and 48 h. The red lines are drawn on the image to aid in visualization of the edges of the gaps. The experiments were independently repeated six times with similar results. Cells were imaged using Keyence BZx-810 microscope and analysis of gap area between cells (μm^2) was quantified using FastTrack A1 software (Ibidi solutions™). Statistical analysis was performed using two-way ANOVA; $^{**}p < 0.01$ and $^{***}p < 0.001$. (D) Cell migration assay using a transwell insert was performed as described in methods. After 18 h, cells in the bottom well were stained with crystal violet and imaged using Keyence BZx-810 microscope. Cells were counted using the Keyence Analyzer software. The experiments were independently repeated three times with similar results. Statistical analysis was performed using one-way ANOVA; $^{***}p < 0.001$. (E) Cell viability was determined using WST1 assay by measuring the formazon dye produced using a plate reader. The experiments were independently repeated four times with similar results. Statistical analysis was performed using *t*-test; $^{***}p < 0.001$. (F) Cell proliferation was determined using BrdU assay by incubating cells in BrdU for 2 h, then fixing and staining with anti-BrdU antibody. Cells were then stained with peroxidase secondary antibody and measured by plate reader. The experiments were independently repeated four times with similar results. Statistical analysis was performed using *t*-test; $^{***}p < 0.001$

Splicing minigenes are valuable molecular tools to identify splice factors that regulate alternative splicing and enable replication of the splicing event without influence of other endogenous factors. PKCδI mRNA is produced by utilization of 5′ splice site I (5′ SSI) and PKCδVIII mRNA is produced by utilization of 5′ splice site II (5′ SSII) on exon 10 of PKCδ pre-mRNA. We previously cloned a human PKCδ splicing minigene to elucidate the mechanisms governing PKCδVIII splicing. Briefly as depicted in schematic of Figure 7C, human PKCδ exon 10 (including both 5′ splice sites) and 200bp of its flanking 3′ and 5′ intronic sequences were cloned into the splicing vector pSPL3 between the splice donor (SD) and splice acceptor (SA) exons (minigene was verified by restriction digestion and sequencing as described in Ref. [14]). To determine that SRSF2 is critical for PKCδVIII expression, the SRSF2 binding site on PKCδ (close proximity to 5′ SSII; denoted by Δ in schematic) was mutated in the minigene (as described in methods and Ref. [14]). The PKCδ splicing minigene (pSPL3_PKCδ) and SRSF2 binding site mutated PKCδ splicing minigene (pSPL3_PKCδ**SRSF2) was transfected into T80, SKOV3 and TOV112D for 24 h. PCR was performed using primers for SD and SA exons. The schematic in Figure 7C shows the primer positions (depicted by arrows on SD and SA exons) and the expected spliced products. Splicing of SD to SA exons serves as constitutive splicing control. Results (Figure 7C) demonstrate that the ovarian cancer cell lines SKOV3 and TOV112D showed increased utilization of 5′ splice site II (which produces PKCδVIII mRNA) in the splicing minigene compared to T80 cells. Further, mutation of the SRSF2 binding site on the splicing minigene significantly decreased utilization of 5′ splice site II in T80, SKOV3, and TOV112D. Interestingly in T80 and TOV112D, the mutated pSPL3_PKCδ**SRSF2 minigene showed a concurrent increase in utilization of 5′ splice site I, showing that a change in balance of bound splice factors in these cells promoted the alternate splicing event. These results show that the increased expression of PKCδVIII in ovarian cancer cell lines SKOV3 and TOV112D is regulated by splice factor SRSF2.

Finally, to validate that SRSF2 binding regulates PKCδVIII expression, we used 2′-methoxy-ethyl-modified (2′MOE), RNAse-H-resistant antisense oligonucleotides. We previously identified and validated an antisense oligonucleotide spanning the SRSF2 binding site[14] which inhibits binding of SRSF2 to exon 10 of PKCδVIII pre-mRNA. 50nM SRSF2 site antisense oligonucleotide (ASO) was transfected into SKOV3 ($SKOV3_{ASO}$) and TOV112D ($TOV112D_{ASO}$) cells or nonspecific scrambled antisense oligonucleotide (control) was transfected for 24 h. RNA was isolated and real-time SYBR Green PCR was performed using primers specific for PKCδI and PKCδVIII. Results (Figure 7D) demonstrate that ASO masking SRSF2 binding site decreased PKCδVIII levels in SKOV3 and TOV112D; the levels of PKCδI or SRSF2 did not change with ASO treatment.

3.12 | Ovarian cancer tissue explants show increased expression of PKCδVIII compared to normal ovarian tissue

To validate our findings in human ovarian explants, we analyzed the expression profile of PKCδVIII using TissueScan ovarian cancer tissue array from Origene Technologies (catalog # HORT103). This array comprises

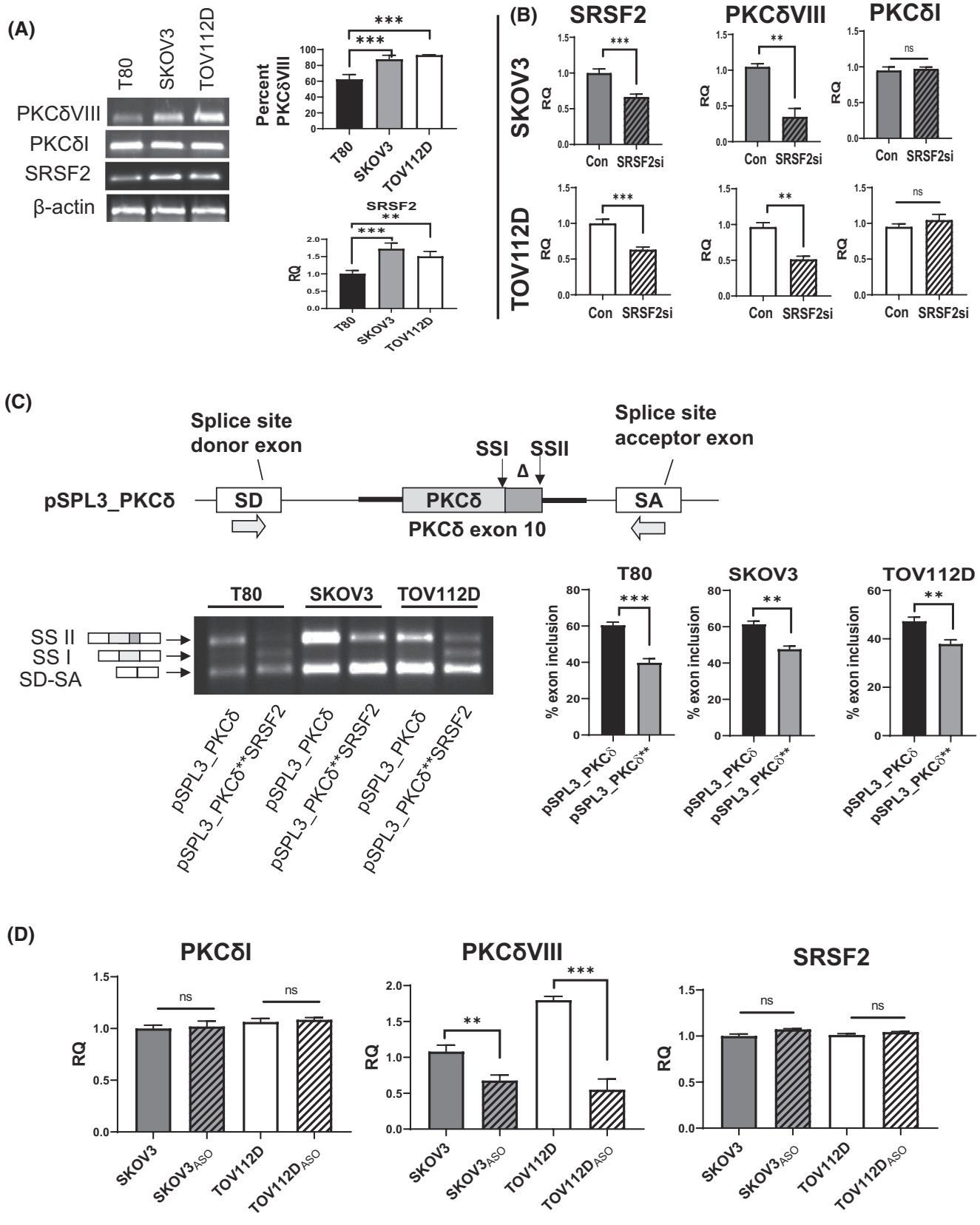

of normal (Stage 0) and tumor samples (Stage I-IV) from individual patients. The cDNA was analyzed using SYBR Green qPCR in triplicate, normalized with β-actin and absolute quantification (AQ) was calculated from the PKCδVIII standard curve. The results (Figure 8A,B) show a dramatically higher level of expression of PKCδVIII across all grades of tumor (Stages I-IV) compared to normal (Stage 0). These results indicate that PKCδVIII is a

FIGURE 7 Alternative splicing of PRKCD gene is regulated by SRSF2 in ovarian cells. (A) RNA was isolated from T80, SKOV3, and TOV112D ovarian cells and PCR was performed using primers for PKCδI, PKCδVIII or SRSF2. PCR products were separated on a 1% agarose gel and visualized using ethidium bromide. The experiments were independently repeated four times with similar results. Graphs show relative quantification of densitometric analysis of SRSF2 normalized to β-actin or percent PKCδVIII (PKCδVIII expression in total PKCδ) was calculated using the following equation: percent PKCδVIII = [PKCδVIII / (PKCδVIII + PKCδI)] × 100. Statistical analysis was performed using *t*-test; $^{**}p < 0.01$ and $^{***}p < 0.001$. (B) 50 nM of SRSF2 specific siRNA was transfected in SKOV3 ($SKOV3_{SRSF2si}$) and TOV112D ($TOV112D_{SRSF2si}$) or 50 nM control siRNA (control) was transfected into the cells for 48 h. RNA was isolated and Real-time SYBR Green qPCR analysis using primers specific to PKCδVIII, PKCδI, SRSF2, and β-actin. Graphs show relative quantification of PKCδI, PKCδVIII, and SRSF2 normalized to β-actin with control set as reference. The experiments were independently repeated four times with similar results. Statistical analysis was performed using one-way ANOVA; $^{**}p < 0.01$, $^{***}p < 0.001$, and ns = not significant. (C) Schematic of PKCδ splicing minigene (pSPL3_PKCδ) with PKCδ exon10 containing 5′ splice site I (5′SSI) and 5′ splice site II (5′SSII) cloned between constitutive splicing donor (SD) and splice acceptor (SA) exons. The SRSF2 binding site on PKCδ exon 10 (close proximity to 5′ SSII; denoted by Δ in schematic) was mutated to generate pSPL3_PKCδ**SRSF2. T80, SKOV3, and TOV112D were transfected with pSPL3_PKCδ or pSPL3_PKCδ**SRSF2 for 24 h. RNA was isolated and PCR was performed using primers specific to SD and SA exons (indicated by arrows in schematic of minigene). The expected products are shown as SD-SA (constitutive splicing), SSI (inclusion of exon 10 using 5′ splice site I which produces PKCδI), and SSII (inclusion of exon 10 using 5′ splice site II which produces PKCδVIII). The PCR products were separated on 1% agarose gel and visualized with ethidium bromide. Densitometric analysis of individual band normalized to SDSA product was performed. The experiments were independently repeated four times with similar results. Graphs show percent use of 5 ′splice site II for exon inclusion using the equation: % exon inclusion = [SSII / (SSII + SDSA)] × 100%. Statistical analysis was performed using *t*-test; $^{**}p < 0.01$ and $^{***}p < 0.001$. (D) 2′-methoxy-ethyl-modified antisense oligonucleotide that masks SRSF2 binding site (ASO) on PKCδVIII exon 10 was transfected in SKOV3 ($SKOV3_{ASO}$) and TOV112D ($TOV112D_{ASO}$) or nonspecific ASO (control) for 48 h. RNA was isolated and Real-time SYBR Green qPCR was performed using primers specific for PKCδVIII, PKCδI, SRSF2, and β-actin. The experiments were independently repeated four times with similar results. Graphs show relative quantification of each gene normalized to β-actin with control set as reference. Statistical analysis was performed using *t*-test; $^{**}p < 0.01$, $^{***}p < 0.001$, and ns not significant

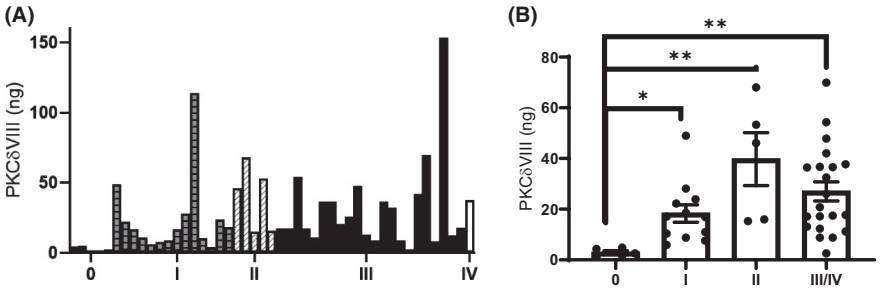

FIGURE 8 PKCδVIII is increased in ovarian tissue explants. (A) TissueScan ovarian cancer array (Origene) was analyzed by Real-time SYBR Green qPCR. For absolute quantification, a standard curve was generated for PKCδVIII. Absolute quantification of PKCδVIII expression levels (ng) was calculated by normalizing the values to β-actin. (B) Ovarian cancer samples were sorted by stage with normal samples as stage 0 and ovarian cancer tumor samples as stages I – IV; stage III/IV were combined. Statistical analysis was performed for stage 0 vs stages I, II or III/IV using one-way ANOVA; $^{*}p < 0.05$ and $^{**}p < 0.01$

viable target to develop therapies for treatment of ovarian cancer.

4 | DISCUSSION

An important mechanism of regulating gene expression is alternative splicing which expands the coding capacity of a single gene to produce different proteins with distinct functions.[17] Sequencing of the human genome predicts >90% of genes are alternatively spliced. Alternative splicing can occur through various mechanisms such as exon skipping, exon inclusion, alternative 3′ splice site usage, alternative 5′ splice site usage, or alternative polyadenylation site usage. Splicing of exons is modulated by *trans*-factors (splice factors) recognizing the *cis*-elements on the pre-mRNA and this mechanism is tightly regulated. Under normal conditions, alternative splicing is tissue-specific, developmental-specific or hormone sensitive. However, mutations in a gene on the cis-elements that bind to splice factors can result in alternative splicing and production of proteins that causes diseases such as spinal muscular atrophy and frontotemporal dementia with parkinsonism linked to chromosome 17 (FTDP-17).[18,19] In other

scenarios such as cancer or diabetes, the disease causes an increase in expression of splice factors or its phosphorylation states which then results in tighter binding of the splice factor to the *cis*-element thereby increasing the expression of specific splice variants. Examples of alternative splicing in cancer include p53 and estrogen receptor genes in breast cancer[20,21] and Bclx in nonsmall cell lung cancer (NSCLC).[22] In this study, we have demonstrated the novel presence of the pro-survival, alternatively spliced PKCδVIII in human ovarian cells. Further, we demonstrated that the expression of PKCδVIII is significantly increased in ovarian cancer, compared to normal ovarian cells. Using splicing minigenes and knockdown studies, we show that alternative splicing of PKCδVIII is regulated by splice factor SRSF2 in ovarian cells. SRSF2 is expressed at high levels in ovarian cancer cells SKOV3 and TOV112D resulting in the increased expression of PKCδVIII.

We previously demonstrated that overexpression of PKCδVIII increases the human telomerase reverse transcriptase (hTERT) expression and increases telomerase activity.[23] Telomerase adds six nucleotide repeats at the end of telomeres to maintain chromosome length. We had demonstrated that high expression of PKCδVIII leads to lower senescence and indicated increased growth potential. In this study, our results demonstrate that PKCδVIII regulates the expression of Bcl2 and overexpression of PKCδVIII affects cell survival and proliferation in ovarian cells. Other groups[24–26] have previously shown that hTERT expression increased the expression of Bcl2 conferring resistance to apoptosis. The role of Bcl2 in promoting cell survival in tumors and hematological malignancies has been extensively studied. It is established that Bcl2 and its family of proteins are critical to tumor development, maintenance as well as resistance to cancer drugs. Our results show TOV112D cells have marked elevated levels of PKCδVIII and Bcl2 in concurrence with a previous study that showed high levels of Bcl2 in TOV112D.[27] Cisplatin is a first-line platinum-based drug used for the treatment of ovarian cancer. Wu et al have reported that TOV112D have acquired cisplatin resistance due to increased levels of Bcl2.[27] Our results suggest that PKCδVIII may contribute to increased cisplatin resistance in cancer.

Protein kinase CδI, the ubiquitously expressed splice variant predominantly referred to as PKCδ in literature, is proteolytically cleaved at the V3 hinge domain in response to apoptotic stimuli by caspase 3. The cleaved catalytic domain promotes apoptosis in several cellular systems.[28–30] We have demonstrated that in humans, the caspase 3 recognition site in the hinge domain is disrupted by inclusion of 31 amino acids due to alternative splicing generating PKCδVIII. We have demonstrated that PKCδVIII independently functions to promote survival in neuronal cells.[4] Here, our results showed increased expression of PKCδVIII in ovarian cancer cells and thus, we sought to elucidate its function. Using robust cellular and molecular techniques, we have established that PKCδVIII promotes cellular survival and proliferation in ovarian cancer cells and additionally established the mechanism by which expression of PKCδVIII is increased in ovarian cancer cells. Our results showed that depletion of PKCδVIII in ovarian cancer cells also reduced their migration. There are several other assays that measure cancer cell invasion, adhesion and motility that determine cancer progression. We are pursuing this separately in conjunction with *in vivo* extrapolations while this project focused on the mechanisms underlying increased PKCδVIII expression.

PKC isozymes have a significant role in signaling cascades in cancers as well as metabolic diseases. Earlier publications have showed the aberrant expression of PKC isoforms such as PKCα, PKCβ, PKCε, PKCδ, and PKCι in ovarian cancer cells[31–39] and demonstrated their roles either as tumor suppressers or as an oncogenic kinases. PKCδ has been reported as promoting apoptosis[32,40] as well as promoting tumor growth and metastasis.[6,41] A significant aspect of understanding opposing roles is the presence of alternatively spliced variants of PKCδ that were not evaluated in these previous studies. The tumor suppressor role of PKCδ in literature may be explained by the presence of the pro-apoptotic PKCδI splice variant. Other signaling kinases such as AKT, CLK are upregulated in cancer which also leads to hyper-phosphorylation of splice factors and changes in alternative splicing. It is also reported that AKT phosphorylates Bad to promote its dissociation from Bcl2 thereby inducing cell survival in cancer cells.[42–44] The regulation of expression of Bcl2 by PKCδVIII may be at the transcriptional level, posttranscriptional regulation via splice factors or rate of turnover. This avenue is being investigated in our lab. Our results show that overexpression of PKCδVIII causes dissociation of Bcl2- Bad complex. We detected phosphorylation on S112 on Bad in T80 which is increased with overexpression of PKCδVIII. However, in SKOV3 and TOV112D cells S112 phosphorylation was low; but we detected high levels of S136 phosphorylation of Bad and did not observe any direct effects of knockdown of PKCδVIII on phosphorylation of S136 on Bad indicating that Bad phosphorylation may not be a direct mechanism through which PKCδVIII promotes survival in ovarian cancer cells. In our co-immunoprecipitation assays, we could not get a robust band of Bad in the Western blot within Bcl2 or Bcl-xL immunoprecipitations. This suggests that the epitope of the Bcl2 and Bcl-xL antibodies used in the immunoprecipitations was in the proximity of Bad binding site. However, immunoprecipitation with Bad followed by western blot analysis showed association with Bcl2 and PKCδVIII. Our

results demonstrate that PKCδVIII increases expression of Bcl2 and further PKCδVIII is a strong binding partner of Bcl2-Bcl-xL complex thereby promoting pro-survival pathways in ovarian cancer cells. Our results show localization of PKCδVIII is distributed between the cytoplasm and perinuclear region in T80 cells while PKCδVIII was detected predominantly in the perinuclear region and nucleus in the cancer cell lines SKOV3 and TOV112D. Previous study[45] has shown that a nuclear localization signal of six basic amino acids is present on the C terminus of PKCδ. These amino acids are conserved in PKCδVIII and likely contribute to the perinuclear and nuclear localization of PKCδVIII.

Our results in human ovarian tissue samples validated that dramatically elevated levels of PKCδVIII are present in ovarian cancer compared to normal ovarian tissue. Several publications have discussed the role of PKCδ in cancer; however, this is the first report demonstrating the role of an alternatively spliced variant, PKCδVIII, in ovarian cancer. Our results underscore the importance of signaling kinases and their role in the cancer microenvironment and further demonstrates that targeting a pivotal signaling kinase is a robust approach to attenuate increased cancer cell survival. Our data using antisense oligonucleotides (ASO) demonstrate that the levels of PKCδVIII can be modulated by ASOs in ovarian cancer. This splice variant-specific modulation is highly significant as it enables translation of the therapeutic into clinical use where it could possibly be combined with other chemotherapeutic agents to combat complex cancers. ASOs have been successfully used[46] in treatment of diseases such as Duchenne muscular dystrophy,[47,48] spinal muscular atrophy,[49] familial hypercholesterolemia.[50] The data presented here demonstrate that the signaling kinase PKCδVIII is a viable target to develop therapeutics to combat progression of ovarian cancer. On a broader level, the splice variant PKCδVIII is specific to humans (the mouse homolog is PKCδII with distinct genetic sequence) and is also expressed in other tissues such as adipose and neuronal as demonstrated by us.[4,51] PKCδVIII promotes survival and its elevated expression may indicate a disease state such as cancer or obesity. We have identified and elucidated the function of the human specific PKCδVIII splice variant in ovarian cells which will significantly aid researchers to develop therapies that can be translated into clinical studies for treatment of ovarian cancer patients.

ACKNOWLEDGMENTS

This work was supported by the Department of Veterans Affairs VAMR I01BX003836 (NAP) and VA RCS IK6BX005387 (NAP). This work does not reflect the view or opinion of the James A. Haley VA Hospital nor the US Government.

CONFLICT OF INTEREST

The authors declare no conflict of interest with regard to this manuscript.

AUTHOR CONTRIBUTIONS

R.S. Patel and R. Rupani are the co-first authors; R.S. Patel designed and performed the majority of experiments; R. Rupani initiated the project and performed the research; S. Impreso performed the research and analyzed the data; A. Lui analyzed the data and drafted the manuscript; N.A. Patel designed the research, analyzed the data, wrote the manuscript, and obtained the funding.

ORCID

Niketa A. Patel https://orcid.org/0000-0003-4811-8596

REFERENCES

1. Jemal A, Siegel R, Ward E, Murray T, Xu J, Thun MJ. Cancer statistics, 2007. *CA Cancer J Clin*. 2007;57:43-66.
2. Jain K, Basu A. Protein kinase C-epsilon promotes EMT in breast cancer. *Breast Cancer (Auckl)*. 2014;8:61-67.
3. Kang JH, Asai D, Toita R, Kitazaki H, Katayama Y. Plasma protein kinase C (PKC)alpha as a biomarker for the diagnosis of cancers. *Carcinogenesis*. 2009;30:1927-1931.
4. Jiang K, Apostolatos AH, Ghansah T, et al. Identification of a novel antiapoptotic human protein kinase C delta isoform, PKCdeltaVIII in NT2 cells. *Biochemistry*. 2008;47:787-797.
5. Patel NA, Song S, Cooper DR. PKCdelta alternatively spliced isoforms modulate cellular apoptosis in retinoic-induced differentiation of human NT2 cells and mouse embryonic stem cells. *Gene Expr*. 2006;13:73-84.
6. Baek JH, Yun HS, Kwon GT, et al. PLOD3 suppression exerts an anti-tumor effect on human lung cancer cells by modulating the PKC-delta signaling pathway. *Cell Death Dis*. 2019;10:156.
7. Hou J, Wang Z, Xu H, et al. Stanniocalicin 2 suppresses breast cancer cell migration and invasion via the PKC/claudin-1-mediated signaling. *PLoS One*. 2015;10:e0122179.
8. Chen Z, Forman LW, Williams RM, Faller DV. Protein kinase C-delta inactivation inhibits the proliferation and survival of cancer stem cells in culture and in vivo. *BMC Cancer*. 2014;14:90.
9. Fujii T, Garcia-Bermejo ML, Bernabo JL, et al. Involvement of protein kinase C delta (PKCdelta) in phorbol ester-induced apoptosis in LNCaP prostate cancer cells. Lack of proteolytic cleavage of PKCdelta. *J Biol Chem*. 2000;275:7574-7582.
10. Shanmugam M, Krett NL, Maizels ET, Murad FM, Rosen ST, Hunzicker-Dunn M. A role for protein kinase C delta in the differential sensitivity of MCF-7 and MDA-MB 231 human breast cancer cells to phorbol ester-induced growth arrest and p21(WAFI/CIP1) induction. *Cancer Lett*. 2001;172:43-53.
11. Yuan J, Lan H, Jiang X, Zeng D, Xiao S. Bcl2 family: novel insight into individualized therapy for ovarian cancer (review). *Int J Mol Med*. 2020;46:1255-1265.
12. Bansal N, Marchion DC, Bicaku E, et al. BCL2 antagonist of cell death kinases, phosphatases, and ovarian cancer sensitivity to cisplatin. *J Gynecol Oncol*. 2012;23:35-42.

13. Risnayanti C, Jang YS, Lee J, Ahn HJ. PLGA nanoparticles co-delivering MDR1 and BCL2 siRNA for overcoming resistance of paclitaxel and cisplatin in recurrent or advanced ovarian cancer. *Sci Rep*. 2018;8:7498.
14. Apostolatos H, Apostolatos A, Vickers T, et al. Vitamin A metabolite, all-trans-retinoic acid, mediates alternative splicing of protein kinase C deltaVIII (PKCdeltaVIII) isoform via splicing factor SC35. *J Biol Chem*. 2010;285:25987-25995.
15. Kelly PN, Strasser A. The role of Bcl-2 and its pro-survival relatives in tumourigenesis and cancer therapy. *Cell Death Differ*. 2011;18:1414-1424.
16. Liang CC, Park AY, Guan JL. In vitro scratch assay: a convenient and inexpensive method for analysis of cell migration in vitro. *Nat Protoc*. 2007;2:329-333.
17. Hastings ML, Krainer AR. Pre-mRNA splicing in the new millennium. *Curr Opin Cell Biol*. 2001;13:302-309.
18. Grover A, Houlden H, Baker M, et al. 5' splice site mutations in tau associated with the inherited dementia FTDP-17 affect a stem-loop structure that regulates alternative splicing of exon 10. *J Biol Chem*. 1999;274:15134-15143.
19. Pistoni M, Ghigna C, Gabellini D. Alternative splicing and muscular dystrophy. *RNA Biol*. 2010;7:441-452.
20. Jolly KW, Malkin D, Douglass EC, Brown TF, Sinclair AE, Look AT. Splice-site mutation of the p53 gene in a family with hereditary breast-ovarian cancer. *Oncogene*. 1994;9:97-102.
21. Daffada AA, Johnston SR, Nicholls J, Dowsett M. Detection of wild type and exon 5-deleted splice variant oestrogen receptor (ER) mRNA in ER-positive and -negative breast cancer cell lines by reverse transcription/polymerase chain reaction. *J Mol Endocrinol*. 1994;13:265-273.
22. Shultz JC, Vu N, Shultz MD, Mba MU, Shapiro BA, Chalfant CE. The Proto-oncogene PKCiota regulates the alternative splicing of Bcl-x pre-mRNA. *Mol Cancer Res*. 2012;10:660-669.
23. Carter G, Patel R, Apostolatos A, Murr M, Cooper DR, Patel NA. Protein kinase C delta (PKCdelta) splice variant modulates senescence via hTERT in adipose-derived stem cells. *Stem Cell Investig*. 2014;1:3.
24. Liu L, Liu Y, Zhang T, et al. Synthetic Bax-Anti Bcl2 combination module actuated by super artificial hTERT promoter selectively inhibits malignant phenotypes of bladder cancer. *J Exp Clin Cancer Res*. 2016;35:3.
25. Vinci S, Giannarini G, Selli C, et al. Quantitative methylation analysis of BCL2, hTERT, and DAPK promoters in urine sediment for the detection of non-muscle-invasive urothelial carcinoma of the bladder: a prospective, two-center validation study. *Urol Oncol*. 2011;29:150-156.
26. Bermudez Y, Erasso D, Johnson NC, Alfonso MY, Lowell NE, Kruk PA. Telomerase confers resistance to caspase-mediated apoptosis. *Clin Interv Aging*. 2006;1:155-167.
27. Wang J, Zhou JY, Zhang L, Wu GS. Involvement of MKP-1 and Bcl-2 in acquired cisplatin resistance in ovarian cancer cells. *Cell Cycle*. 2009;8:3191-3198.
28. Emoto Y, Manome Y, Meinhardt G, et al. Proteolytic activation of protein kinase C delta by an ICE-like protease in apoptotic cells. *Embo J*. 1995;14:6148-6156.
29. Reyland ME, Anderson SM, Matassa AA, Barzen KA, Quissell DO. Protein kinase C delta is essential for etoposide-induced apoptosis in salivary gland acinar cells. *J Biol Chem*. 1999;274:19115-19123.
30. Mizuno K, Noda K, Araki T, et al. The proteolytic cleavage of protein kinase C isotypes, which generates kinase and regulatory fragments, correlates with Fas-mediated and 12-O-tetradecanoyl-phorbol-13-acetate-induced apoptosis. *Eur J Biochem*. 1997;250:7-18.
31. Zhao LJ, Xu H, Qu JW, Zhao WZ, Zhao YB, Wang JH. Modulation of drug resistance in ovarian cancer cells by inhibition of protein kinase C-alpha (PKC-alpha) with small interference RNA (siRNA) agents. *Asian Pac J Cancer Prev*. 2012;13:3631-3636.
32. Wang F, Wang Z, Gu X, Cui J. miR-940 upregulation suppresses cell proliferation and induces apoptosis by targeting PKC-delta in ovarian cancer OVCAR3 cells. *Oncol Res*. 2017;25:107-114.
33. Tyagi K, Roy A. Evaluating the current status of protein kinase C (PKC)-protein kinase D (PKD) signalling axis as a novel therapeutic target in ovarian cancer. *Biochim Biophys Acta Rev Cancer*. 2021;1875:188496.
34. Masanek U, Stammler G, Volm M. Modulation of multidrug resistance in human ovarian cancer cell lines by inhibition of P-glycoprotein 170 and PKC isoenzymes with antisense oligonucleotides. *J Exp Ther Oncol*. 2002;2:37-41.
35. Diaz-Cueto L, Arechavaleta-Velasco F, Diaz-Arizaga A, Dominguez-Lopez P, Robles-Flores M. PKC signaling is involved in the regulation of progranulin (acrogranin/PC-cell-derived growth factor/granulin-epithelin precursor) protein expression in human ovarian cancer cell lines. *Int J Gynecol Cancer*. 2012;22:945-950.
36. Cartee L, Kucera GL, Nixon JB. The effects of gemcitabine and TPA on PKC signaling in BG-1 human ovarian cancer cells. *Oncol Res*. 1998;10:371-377.
37. Carduner L, Picot CR, Leroy-Dudal J, Blay L, Kellouche S, Carreiras F. Cell cycle arrest or survival signaling through alphav integrins, activation of PKC and ERK1/2 lead to anoikis resistance of ovarian cancer spheroids. *Exp Cell Res*. 2014;320:329-342.
38. Cao Z, Liu LZ, Dixon DA, Zheng JZ, Chandran B, Jiang BH. Insulin-like growth factor-I induces cyclooxygenase-2 expression via PI3K, MAPK and PKC signaling pathways in human ovarian cancer cells. *Cell Signal*. 2007;19:1542-1553.
39. Al-Alem LF, McCord LA, Southard RC, Kilgore MW, Curry TE Jr. Activation of the PKC pathway stimulates ovarian cancer cell proliferation, migration, and expression of MMP7 and MMP10. *Biol Reprod*. 2013;89:73.
40. Weichert W, Gekeler V, Denkert C, Dietel M, Hauptmann S. Protein kinase C isoform expression in ovarian carcinoma correlates with indicators of poor prognosis. *Int J Oncol*. 2003;23:633-639.
41. Mauro LV, Grossoni VC, Urtreger AJ, et al. PKC Delta (PKCdelta) promotes tumoral progression of human ductal pancreatic cancer. *Pancreas*. 2010;39:e31-e41.
42. Kumar MV, Shirley R, Ma Y, Lewis RW. Role of genomics-based strategies in overcoming chemotherapeutic resistance. *Curr Pharm Biotechnol*. 2004;5:471-480.
43. Daragmeh J, Barriah W, Saad B, Zaid H. Analysis of PI3K pathway components in human cancers. *Oncol Lett*. 2016;11:2913-2918.
44. Pilling AB, Hwang C. Targeting prosurvival BCL2 signaling through Akt blockade sensitizes castration-resistant prostate cancer cells to enzalutamide. *Prostate*. 2019;79:1347-1359.
45. DeVries TA, Neville MC, Reyland ME. Nuclear import of PKCdelta is required for apoptosis: identification of a novel nuclear import sequence. *EMBO J*. 2002;21:6050-6060.

46. Tang Z, Zhao J, Pearson ZJ, Boskovic ZV, Wang J. RNA-targeting splicing modifiers: drug development and screening assays. *Molecules*. 2021;26.
47. Syed YY. Eteplirsen: first global approval. *Drugs*. 2016;76: 1699-1704.
48. Hanson B, Wood MJA, Roberts TC. Molecular correction of Duchenne muscular dystrophy by splice modulation and gene editing. *RNA Biol*. 2021;1-15.
49. Chiriboga CA. Nusinersen for the treatment of spinal muscular atrophy. *Expert Rev Neurother*. 2017;17:955-962.
50. Waldmann E, Vogt A, Crispin A, Altenhofer J, Riks I, Parhofer KG. Effect of mipomersen on LDL-cholesterol in patients with severe LDL-hypercholesterolaemia and atherosclerosis treated by lipoprotein apheresis (The MICA-Study). *Atherosclerosis*. 2017;259:20-25.
51. Carter G, Apostolatos A, Patel R, et al. Dysregulated alternative splicing pattern of PKC during differentiation of human preadipocytes represents distinct differences between lean and obese adipocytes. *ISRN Obesity*. 2013;2013:9.

How to cite this article: Patel RS, Rupani R, Impreso S, Lui A, Patel NA. Role of alternatively spliced, pro-survival Protein Kinase C delta VIII (PKCδVIII) in ovarian cancer. *FASEB BioAdvances*. 2022;4:235–253. doi:10.1096/fba.2021-00090